J. Bangladesh Acad. Sci. 47(1); 127-137: June 2023 DOI: https://doi.org/10.3329/jbas.v47i1.63983

Journal of Bangladesh Academy of Sciences

Journal homepage: http://www.bas.org.bd/publications/jbas.html

Research Article

MHD convection in a square cavity with a heated cone: Effects of magnetic field and cone orientation

Saika Mahjabin and Md. Abdul Alim[1]

Department of Mathematics, National University, Gazipur, Bangladesh

ARTICLE INFO

Article History

Received: 21 December 2022
Revised: 05 June 2023
Accepted: 11 June 2023

Keywords: MHD free convection, Hartmann number, Square cavity, Heated cone, Finite element method

ABSTRACT

This paper presents a study on the influence of Magnetic Force impressed upon MHD fluid contained in a square cavity with a heated cone. The novelty of this work includes a heated cone whose orientation is varied at different angles. Calculations are performed for Prandtl number Pr = 0.71; Rayleigh number Ra = 10, 1000, and 100000; and Hartmann number Ha = 0, 50, and 100. The results are illustrated with streamlines, isotherms, and other relevant plots. It is observed that the influence of Ha becomes more noticeable with increasing Ra. Ha affects the flow by retarding the fluid movement and thus affects convective heat transfer. It is also observed that the cone orientation influences both fluid circulation and heat transfer. At high Ra, the vertical orientation of the cone resulted in lower heat flux than the left/right orientations. Also, under the same condition, the system remains cooler with the vertical cone at lower Ha, but becomes hotter after a certain value of Ha. These findings have practical design implications.

Introduction

The thermal behavior of Magneto-hydro-dynamic (MHD) fluids is an interesting subject. It has both theoretical and practical interests. Some practical applications include liquid metals, plasma, and high-velocity objects. The cone is an important shape, frequently seen in connection with fluid motion. The air molecules break apart at hypersonic speeds, producing electrically charged plasma around the aircraft (NASA 2022). Conical objects are also frequently used in pressure and flow control devices. The square is a basic shape, which provides scope for a baseline study, which can be extended to other shapes by changing the aspect ratio. For these reasons, square cavities and conical objects are chosen.

Much researched has been published on MHD fluid. Yang (1987), Kulacki et al. (1987), Moreau (1990), Vives and Perry (1987) published reviews on this subject. Many of the works mentioned in these reviews involve MHD fluid in enclosures, while the walls are maintained at different temperatures. The enclosures sometimes also contained objects of various shapes. A few recent works are mentioned next.

Sathiyamoorthy and Chamkha (2012) reported MHD fluid in a square cavity with an impressed magnetic field. The magnetic field strongly influenced the heat transfer regardless of wall heating conditions.

Bakhshan and Ashoori (2012) reported similar findings with a rectangular enclosure Nusselt number increased with Grashof (Gr) and Prandtl (Pr) numbers, indicating better heat transfer, and Hartmann number (Ha) had the opposite effect. Öztop and Al-Salem (2012) included joule heating in their study, along with a magnetic field. In their case, a strong magnetic field slowed the fluid motion and made the thermal

*Corresponding author: <mahjabinsaika.bd@gmail.com>

[1]*Department of Mathematics, Bangladesh University of Engineering & Technology, Dhaka, Bangladesh*

boundary layer thicker. Taghikhani and Chavoshi (2013) considered internal heating also, observing the reduction of convective heat transfer with *Ha*. Bhuiyan et al. (2014) placed a heated square block in the cavity and found that both the position of the block and *Ha* had influenced heat transfer. Hossain et al. (2015) investigated an open square cavity with a heated cylinder. It was found that the heat flux decreased with increasing *Ha*. Thus, the magnetic field had a retarding effect on flow and heat transfer. Ashouri et al. (2014) considered the cavity partially filled with conducting solid square obstacles. They also investigated the effect of the thermal conductivity ratio between the solid and fluid materials for different numbers of solid blocks. It was observed that the Nusselt number varied with solid-to-fluid thermal conductivity ratio, *Ha*, and the number of solid blocks. Hossain et al. (2015) also reported that the temperature and flow fields significantly varied between *Ra* and *Ha*. Mokaddes et al. (2021) investigated Casson fluid in double-lid driven square cavities. They found that the flow strength increases with the Reynolds number (Re) and Casson parameter and decreases with *Ha*. Ciofalo (2023) reported on MHD convection in one-dimensional configuration, i.e., indefinitely long vertical duct. It was shown that the system could be operated in different ways, such as an Electromagnetic pump, MHD generator, or a heat engine, depending on the boundary conditions. Mythreye (2023) studied MHD convection through a porous medium bounded by two vertical walls, together with chemical reactions and radiation. It is reported that velocity decreases with the increase in *Ha*, Chemical reaction parameter, *Kr*, and *Pr*. Bakar et al. (2020) reported the effects of *Ha* on MHD mixed convection in a li-driven rectangular cavity. As *Ha* increases, the flow convection is attenuated, and the heat transfer rate decreases. Goud et al. (2023) investigated the MHD flow of nanofluid on an inclined spinning disk with heat absorption and chemical reaction. The velocity of the fluid decreased with increasing *Ha*. A rise in thermal radiation (*Rd*) causes the temperature graphs to grow substantially, although the concentration profiles exhibit the opposite tendency. The short review presented indicates the number and variations of research works. The studies covered different fluids with different geometries of the cavity, the object inside the cavity, and heating conditions. The most common finding from all these works is that, for MHD fluid, the magnetic force retards fluid flow and hampers heat transfer. However, to the best of the authors' knowledge, the issue of the present work, i.e., the effect of cone orientations, has not been reported.

Model and Mathematical Formulation

The physical model is shown in Fig.1.

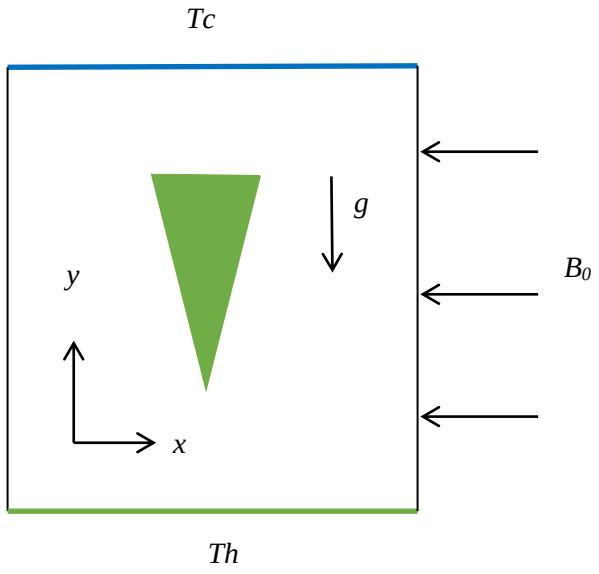

Fig. 1. Schematic diagram of the model

The top wall is held at a lower constant temperature (T_c), and the lower wall is at a higher temperature (T_h). Both the left and right walls are adiabatic. The cone temperature is constant at (T_h). The cone is placed at three angles: i) vertical, ii) left inclined, and iii) right inclined. The magnetic field B_0 acts perpendicularly to the flow.

The density of the fluid varies with the temperature, and other properties remain constant. Radiation and Joule heating are not considered. With these assumptions, we get the following:

i) Conservation of mass $\frac{\partial u}{\partial x} + \frac{\partial v}{\partial y} = 0$ (1)

ii) Conservation of momentum:

ii.a) x-momentum equation $\rho\left(u\frac{\partial u}{\partial x} + v\frac{\partial u}{\partial y}\right) = -\frac{\partial p}{\partial x} + \mu\left(\frac{\partial^2 u}{\partial x^2} + \frac{\partial^2 u}{\partial y^2}\right)$

ii. b) y-momentum equation

$$\rho\left(\mathrm{u}\frac{\partial \mathrm{v}}{\partial \mathrm{x}} + \mathrm{v}\frac{\partial \mathrm{v}}{\partial \mathrm{y}}\right) = -\frac{\partial \mathrm{p}}{\partial \mathrm{y}} + \mu\left(\frac{\partial^2 \mathrm{v}}{\partial \mathrm{x}^2} + \frac{\partial^2 \mathrm{v}}{\partial \mathrm{y}^2}\right) + \rho g\beta\,(T - T_c) - \sigma B_0^2 v$$

iii) Conservation of Energy: $u\frac{\partial T}{\partial x} + v\frac{\partial T}{\partial y} = \alpha\left(\frac{\partial^2 T}{\partial x^2} + \frac{\partial^2 T}{\partial y^2}\right)$

The governing equations are made dimensionless using the following dimensionless variables:

$X = \frac{x}{L}$ $Y = \frac{y}{L}$ $U = \frac{uL}{\alpha}$ $V = \frac{vL}{\alpha}$

$P = \frac{pL^2}{\rho\alpha^2}$ $\theta = \frac{T - T_c}{T_h - T_c}$ $\sigma = \frac{\rho^2\alpha}{L^2}$ $\alpha = \frac{k}{\rho C_p}$

$\nu = \frac{\mu}{\rho}$

Applying these definitions, the following dimensionless equations are obtained.

$$\frac{\partial U}{\partial X} + \frac{\partial V}{\partial Y} = 0$$

$$U\frac{\partial U}{\partial X} + V\frac{\partial U}{\partial Y} = -\frac{\partial P}{\partial X} + Pr\left(\frac{\partial^2 U}{\partial X^2} + \frac{\partial^2 U}{\partial Y^2}\right)$$

$$\mathrm{U}\frac{\partial \mathrm{V}}{\partial \mathrm{X}} + \mathrm{V}\frac{\partial \mathrm{V}}{\partial \mathrm{Y}} = -\frac{\partial \mathrm{P}}{\partial \mathrm{Y}} + \mathrm{Pr}\left(\frac{\partial^2 \mathrm{V}}{\partial \mathrm{X}^2} + \frac{\partial^2 \mathrm{V}}{\partial \mathrm{Y}^2}\right) + \frac{Ra}{Pr}\theta - Ha^2\,\mathrm{Pr}\,V\,U\frac{\partial \theta}{\partial X} + V\frac{\partial \theta}{\partial Y} = \frac{\partial^2 \theta}{\partial X^2} + \frac{\partial^2 \theta}{\partial Y^2}$$

Where,

Prandtl number, $Pr = \frac{\nu}{\alpha}$;

Hartmann number, $Ha^2 = \frac{\sigma B_0^2 L^2}{\mu}$;

Grashof number, $Gr = \frac{g\,\beta\,L^3(T_h - T_c)}{\nu^2}$;

Rayleigh number, $Ra = \frac{g\,\beta\,L^3(T_h - T_c)\,Pr}{\nu^2}$;

Boundary Conditions

After applying the above dimensionless quantities, the dimensionless boundary conditions become:

$U = V = 0,\ \theta = 1$ at the bottom wall and heated conical body

$U = V = 0,\ \theta = 0$ at the top wall

$U = V = 0,\ \frac{\partial \theta}{\partial N} = 0$ at side walls

$P = 0$ Fluid pressure at the inside and on the walls of the cavity

Moreover, μ is the fluid's viscosity, β is the coefficient of thermal expansion, and B_0 is the magnetic force.

Numerical Procedure

The finite element method is used to solve the equations shown above. The detailed procedures of finite elements can be found in the works of Taylor and Hood (1973), Reddy (1993), and Dechaumphai (1999), etc.

Grid Generation

The model is discretized into elements. The governing and boundary equations are applied to each element to get a solution for the entire system. Therefore, the finer the mesh, the more accurate the result. However, finer meshing involves a much greater number of operations and time. Therefore, a reasonable number of elements are taken to obtain results with acceptable accuracy and not over-taxing computer resources or time. This is presented next.

Grid Refinement Check

The accuracy of the finite element method is sensitive to the number of cells or the mesh size. In general, a finer mesh is expected to yield greater accuracy. However, taking finer mesh for a short time is only practical for two reasons. Firstly, more cells result in longer runtime and may overtax the computer's resources. Secondly, adding more cells does not significantly improve the accuracy after a certain number of cells. Therefore, an optimum number of cells should be selected. In this study, the average Nusselt number was calculated for benchmarking accuracy.

The average Nusselt number (Nu) was calculated with different numbers of elements. The results are shown in Fig. 2. It is seen that beyond 8,000 elements, the change in Nu diminishes. Thus, the

mesh with 8,039 elements was chosen. The resulting mesh structure is displayed in Fig.3.

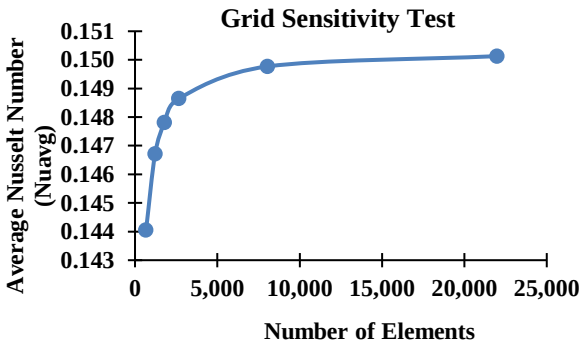

Fig. 2. Grid sensitivity (*Ha* = 0, *Ra* =1E5).

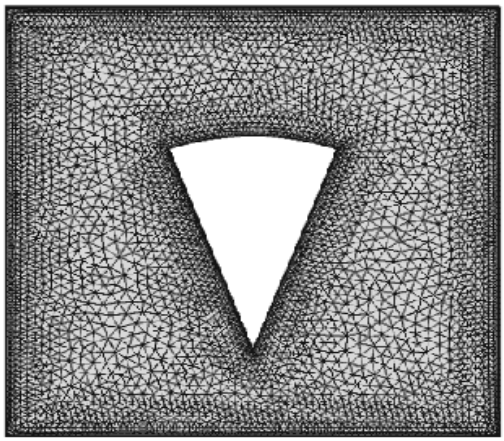

Fig. 3. Mesh with 8,039 elements.

Code Validation

There is no experimental data available to validate our code. Therefore, the only option was to check it against some published numerical results. The code underlying the present model was checked against that of the work of Bhuiyan et al. (2014). Current work involves a conical object in a square cavity, while their work involves a square object placed at different corners. Therefore, we replaced the cone with a heated square object and generated streamlines and isotherms. Fig. 4 shows the comparisons graphically. It is seen that the results are very similar. Thus, our code was validated.

Results and Discussions

The following parameter values were used in the calculations:

Prandtl number *Pr* = 0.71

Rayleigh number *Ra* = 10, 1000, and 100,000;

Hartmann number *Ha* = 0, 50, and 100. The results and discussions are presented in two main segments- ***i) fluid motion and ii) heat transfer***. Only the results involving *Ha* = 0 and 100 are presented for brevity.

i) Fluid Motion Study

The fluid inside the cavity is set in motion by convection. Since it is a closed system, the fluid remains in the cavity and circulates. In a steady-state laminar flow system, fluid particles follow fixed paths, but velocity along a certain arbitrary path may vary. This is best illustrated with streamlines.

Streamlines

Fig. 5 presents streamlines for the three-cone orientations. The parameters are Raleigh number (*Ra*), which represents the degree of fluid movement or circulation, and Hartmann number (*Ha*), which represents the intensity of the magnetic field. It was observed before (Mahjabin and Alim, 2018) that the effect of *Ha* became more noticeable with high *Ra*. Therefore only the results with *Ra* = 100,000 are presented.

The flow patterns for the left and right inclinations of the cone are like a mirror image. At *Ha* = 0, one vortex is created on either side of the cone. Two main and two sub-vortices are seen for the vertical cone.

A color scale indicates fluid velocities. Local fluid velocities are greater while passing through narrow channels, as expected.

At *Ha* = 100, the streamlines for left and right cone positions remained somewhat the same, although the position of the vortex changed. For the vertical position, the sub-vortices disappeared, and the main vortices moved towards the colder surface, i.e., to the top wall. The most important phenomenon, however, is the dramatic reduction of velocity, as shown in the color legend scale next to each figure. For example, for the vertical cone position, the velocity range reduced from 60-10 to 6-1, i.e., a ten-fold reduction was achieved by impressing the magnetic field. Therefore, the effect of *Ha* is to retard fluid movement. The reason can be explained as follows.

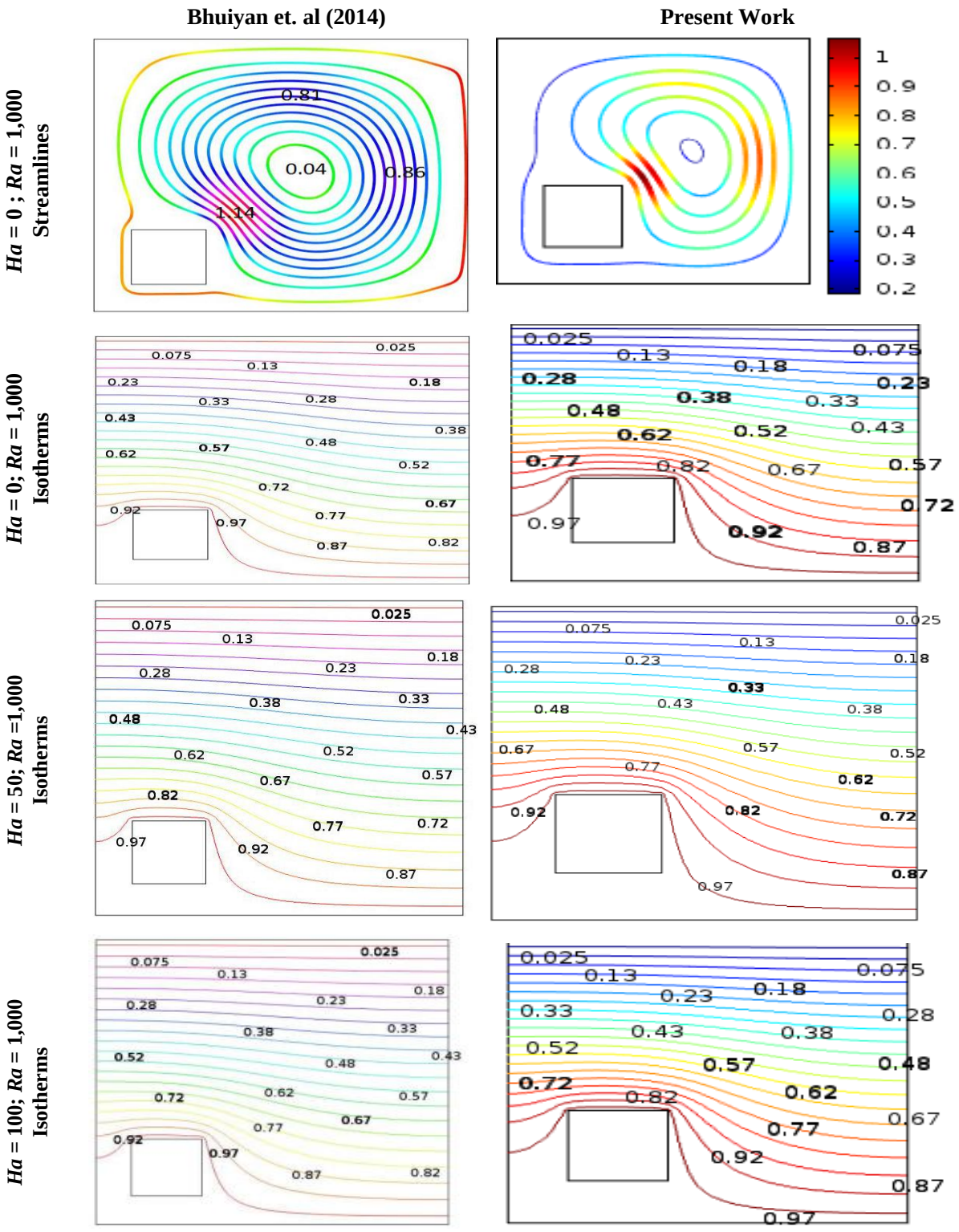

Fig. 4. Code validation: Comparison of results between present work and Bhuiyan et al. (2014)

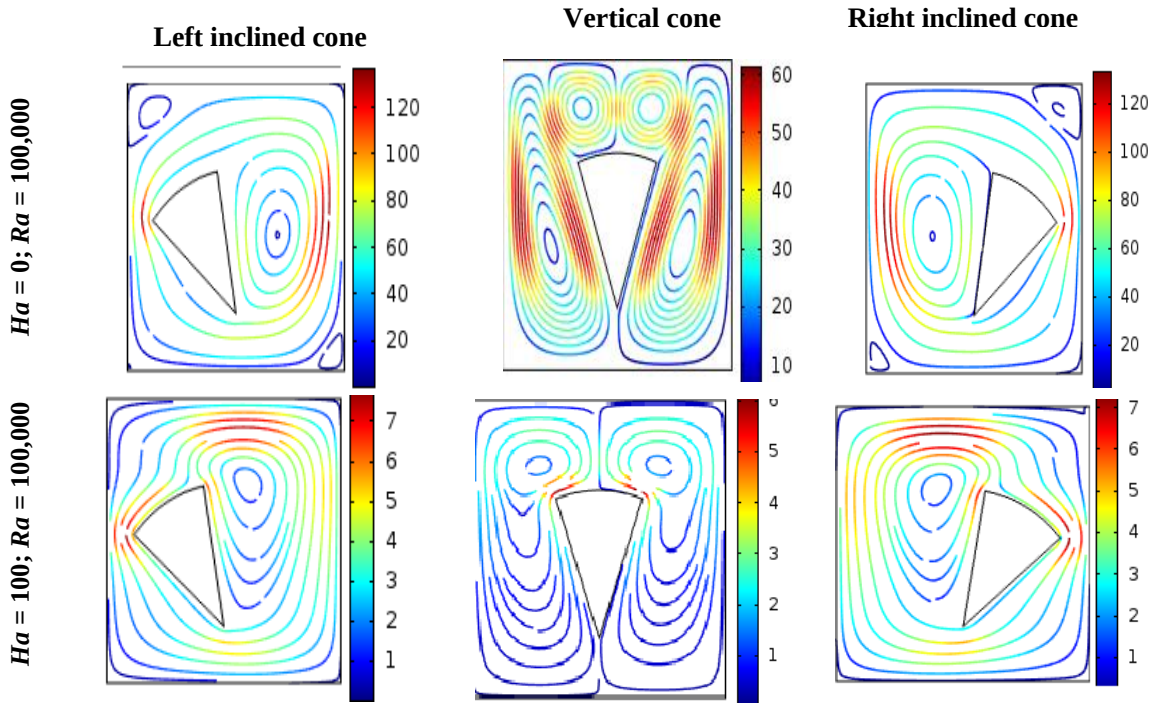

Fig. 5. Streamlines illustrating the effect of *Ha* on fluid movement.

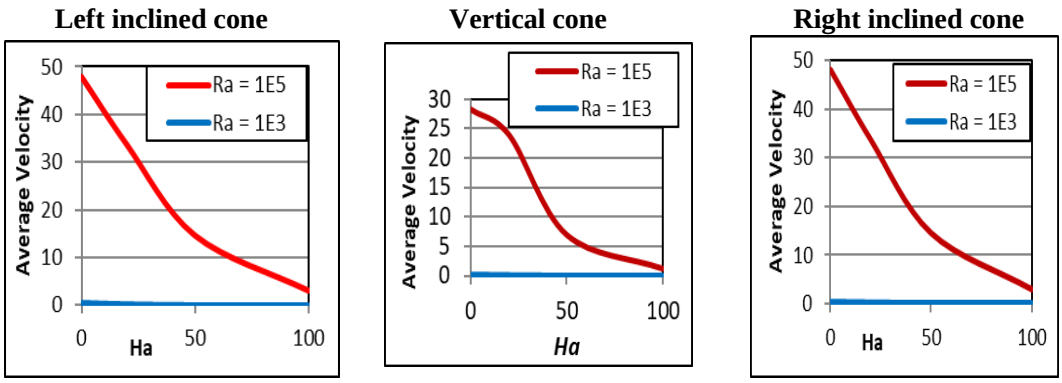

Fig. 6. Volumetric Average velocity for different *Ha* and *Ra.*

Three forces are acting on the system- the body force, which is the weight of the fluid, and it always works downwards. There is buoyancy force, which arises from the density difference of the fluid. The density difference is caused by the heat applied through the bottom wall and from the cone. Hotter fluid is less dense and tends to rise toward the colder region. Denser fluid from the colder region moves downward. Thus, initially, the fluid starts to move at rest, and circulation is established. However, the fluid circulation cannot increase indefinitely. The fluid circulation eventually reaches equilibrium for a given condition, such as at a fixed Ra. The fluid velocity, or the circulation rate, is directly related to the Raleigh number. The greater value of *Ra* implies more circulation and greater fluid velocity. The third force in the system is the magnetic field. When applied to an MHD fluid, it produces a drag-like force called the Lorentz force. It causes a reduction in the fluid velocity.

It should be noted that the fluid must be in motion to manifest any effect of a magnetic force. Thus, greater intensity of the magnetic force (Ha) is expected to slow down the fluid circulation. This physical

explanation applies to all the results presented in the subsequent sections.

Average Velocity

Streamlines indicate the fluid circulation paths and velocity variations, but the average velocity can provide insight into the overall flowing condition in the cavity. Therefore, the average volumetric velocity of the fluid was calculated for each configuration and presented in Fig. 6.

The variation of the volumetric average velocity for the three orientations of the cone is quite similar, although the magnitudes are slightly different. For high *Ra*, the average velocity decreases sharply with increasing *Ha*. For example, for the vertical cone, average velocity is reduced from 28 to 2, i.e., about 14 times reduction was achieved when *Ha* was increased from 0 to 100. This is consistent with previous observations (Fig. 5). The impact of *Ha* at lower *Ra* is not noticeable.

can illustrate. These lines remain fixed for a given configuration and a fixed set of parameters. As mentioned before, the effect of *Ha* is more noticeable with large values of *Ra*. Therefore, only isotherms with *Ra* = 100,000 and *Ha* =0 and 100 are presented in Fig.7. Asymmetric, closely packed isotherms imply uneven and inefficient heat transfer. In contrast, more evenly spaced isotherms indicate smoother temperature distribution and more efficient heat transfer.

Fig. 7 shows isotherms with color shades. Numbers next to the isotherms are dimensionless temperatures. The lighter shades indicate hotter zones.

The isotherms for the left and right inclinations of the cone are like a mirror image and symmetric around the vertical cone. At high *Ra* and zero *Ha*, the lines are distorted and spread across more cavity areas for all three cone positions. The hotter fluid covers lesser parts of the body. With the greater circulation of the

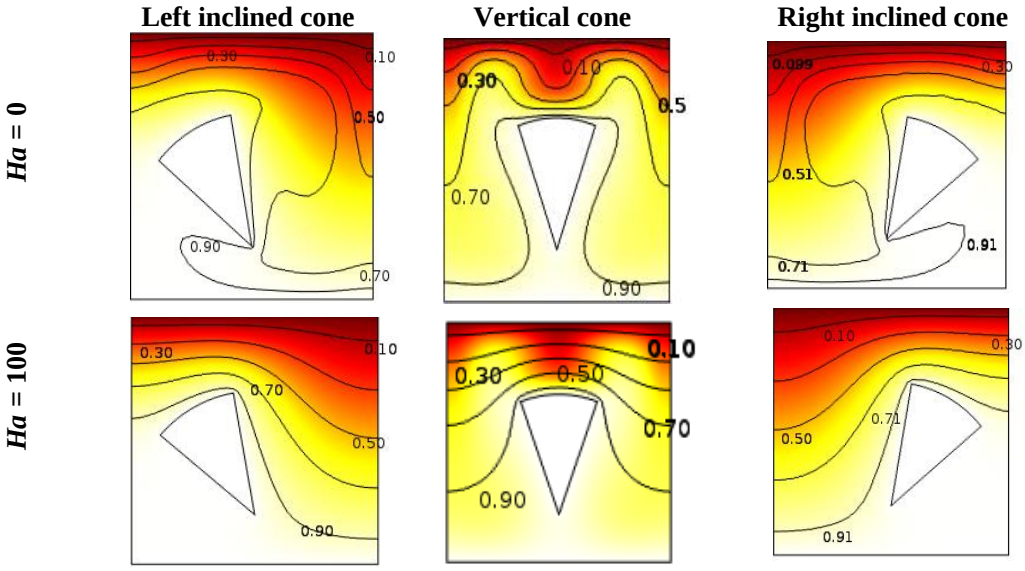

Fig. 7. Isotherms illustrating the effect of *Ha* on temperature distribution (*Ra* = 100,000).

ii) Heat transfer Study

Heat transfer is studied in terms of temperature distribution (isothermal lines), average temperature, local Nusselt number, and Heat flux. These are presented next.

Isotherms

In a steady-state system, the temperature is distributed over the system, which isothermal lines

fluid, heat is carried more efficiently from the hotter to the colder region.

With *Ha* = 100, the isotherms become smoother and more compacted. The hotter fluid covers more portions of the cavity. It means the heat is less efficiently removed from the hotter to the colder

region. Since convective heat transfer mainly depends on fluid movement, any restriction on fluid movement will influence heat transfer. The heat transfer mechanism becomes more like conduction than convection. The temperature distribution thus becomes more even, as seen in the isotherms. It may be inferred that *Ha* retarded both fluid circulation and heat transfer.

Average Temperature

Isotherms indicate the temperature distribution, but the average temperature can provide insight into the heating condition in the cavity. Therefore, the volumetric average temperature of the fluid was calculated for each configuration and presented in Fig. 8.

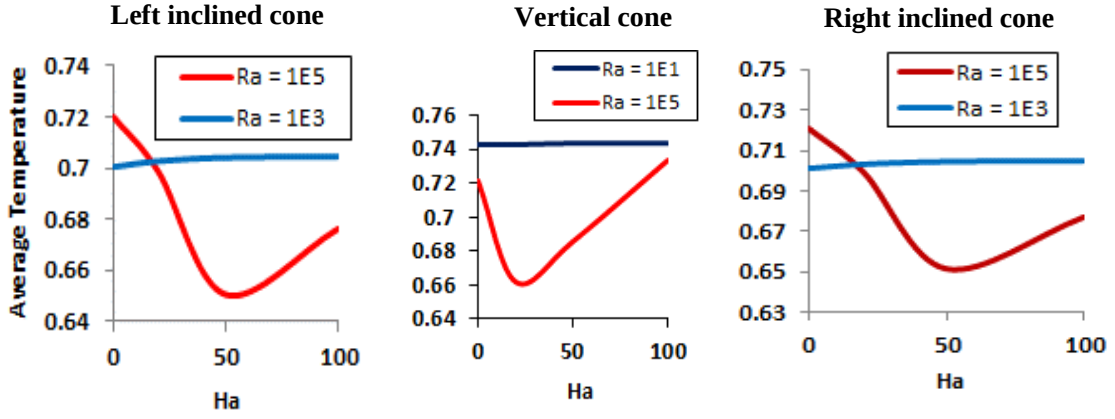

Fig. 8. Volumetric average temperature for different *Ha* and *Ra*.

The average temperature variation for the left and right cone orientations is identical, and for the vertical position, it is somewhat different. For high *Ra*, the average temperature decreases first and then increases with *Ha*. The average temperature remains generally higher for all three orientations for low *Ra* and slightly varies with *Ha*. This observation has practical design implications. For example, if there is a requirement to keep the system cool, the corresponding *Ha* should be applied. *Ha* greater or smaller than this value will make the system hotter.

Nusselt Number

The local and average Nusselt numbers were evaluated *for the vertical cone only*, and the results are shown in Table 1. The average Nusselt Number decreased with increasing *Ha*, indicating a retarding effect on heat transfer.

The local Nusselt number was evaluated along the bottom hot wall and plotted in Fig. 9. It shows *Nu* is lowest at the center. This is consistent because this point is just below the heated cone. Heat transfer should be the minimum between two hot bodies of the same temperature, as indicated by the dip of the curves.

Table 1. Average Nusselt Number

Ha	*Ra*	Nu_{avg}
0	1.00E+05	1.16098
50	1.00E+05	0.45942
100	1.00E+05	0.1793

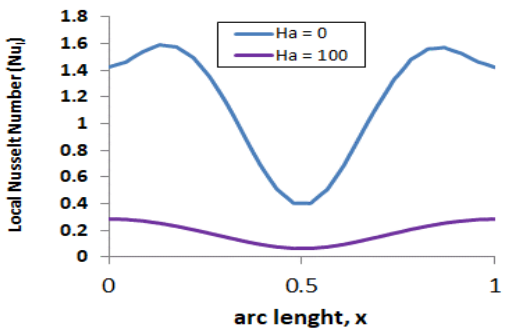

Fig. 9. Local Nusselt number as a function of *Ha* (*Ra* = 1E5)

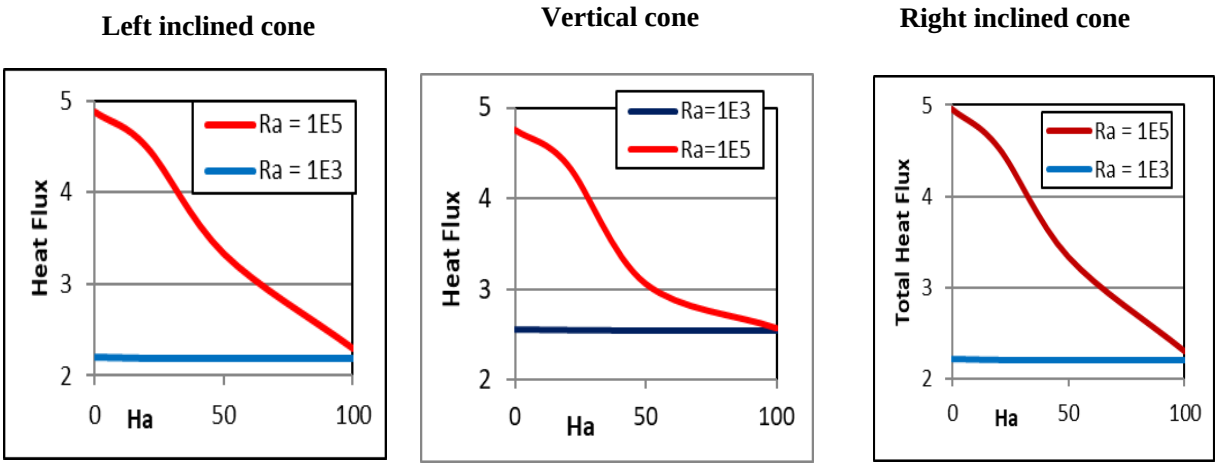

Fig. 10. Heat flux as a function of *Ha* and *Ra*

Heat Flux

The most direct and quantitative study of heat transfer is heat flux, which indicates the amount of heat energy passing through a plane of unit area. It was calculated for a plane adjacent to the top wall of the cavity with different values of *Ha* and *Ra*, and shown in Fig. 10.

The patterns are quite similar for all cone positions for high *Ra*. Heat flux decreases noticeably with *Ha*. For example, for the vertical cone, at *Ra* = 100,000, the heat flux reduced from 4.8 to 2.5 when *Ha* was increased from 0 to 100. The effect of *Ha* at low *Ra* is minimal. However, at low *Ra*, heat flux is greater for the vertical position. This observation is consistent with all previous observations. It is interesting to note that the plots look very similar.

Comparison of Average Velocity

Fig. 11 compares the three curves, representing the volumetric average velocity for the three cone orientations, for a given *Ra* = 100,000 and different *Ha*. At high *Ra* (100,000) and *Ha* = 0, average velocity is about 42% lower for the vertical cone compared to the inclined cones. With increasing *Ra*, this difference diminishes.

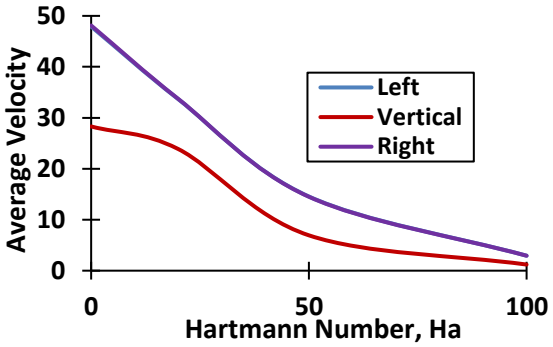

Fig. 11. Effect of cone orientation on average volumetric velocity (*Ra* = 100,000). Note: Left & right orientation produced identical results. Hence the 2 curves merged.

The average velocity variation with *Ha* is identical for the left and right orientation of the cone, while it is somewhat different for the vertical position. In all cases, the average velocities gradually reduce with increasing *Ra*. Most noticeably, the vertical position results in lower average velocity than the inclined positions.

Comparison of Average Temperature

Fig. 12 shows the volumetric average temperature for the three-cone orientations.

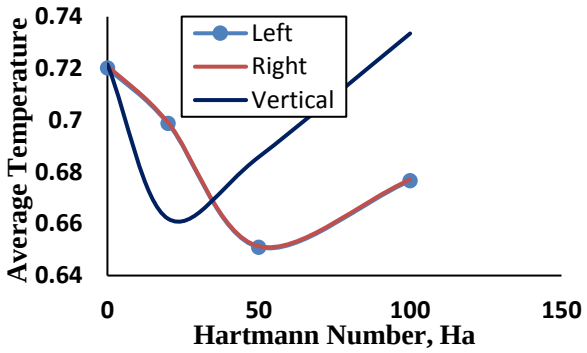

Fig. 12. Effect of cone orientation on volumetric average temperature (*Ra* = 100,000). Note: Left & right orientation produced identical results. Hence the 2 curves merged.

The average temperature variation with *Ha* is identical for the left and right orientation of the cone, while it is noticeably different for the vertical position. In all cases, the temperature decreases first and then increases with *Ha*. For the vertical position, the lowest temperature appears earlier, at a lower *Ha*, and remains lower than the other two curves representing the left and right inclined cone. However, after about *Ha* = 40, the temperature remains higher for the vertical position. The design implication of this phenomenon is that the system will be hotter with the vertical cone for *Ha* > 40.

Comparison of Heat Flux

The effect of orientation on heat flux is shown in Fig. 13.

At lower *Ha*, the left and right orientations of the cone show identical results and indicate a greater heat flux.

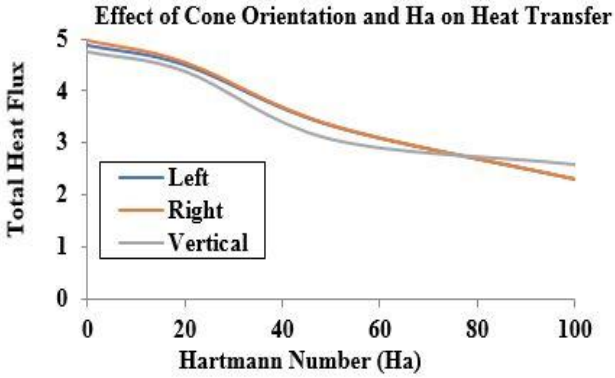

Fig. 13. The effect of orientation on heat flux (*Ra* = 100,000).

The vertical position after about Ha = 80 resulted in greater heat flux. It implies that the system is more efficient for heat transfer with the inclined positions if circulation needs to be high. Otherwise, the vertical position should result in a more efficient system (Fig. 10).

Conclusion

At high *Ra*, fluid particles move at a higher velocity without any magnetic force. Impressing a magnetic field in this situation produced a noticeable effect by slowing the fluid movement. For example, in the case of the vertical cone, with Ra held at 100,000, the fluid velocity reduced almost 10 times when *Ha* was increased from 0 to 100. The average velocity is reduced from 28 to 2, i.e., about 14 times reduction was achieved when *Ha* was increased from 0 to 100 for the vertical cone. The velocity reduction effect caused by *Ha* also affects the temperature distribution and heat flux. For example, at Ra = 100,000 for the vertical cone, the heat flux reduced from 4.8 to 2.5 when *Ha* increased from 0 to 100. The cone's orientation also significantly impacts the average velocity, temperature, and heat flux. At *Ra*=100,000 and *Ha* = 0, the average velocity is about 42% lower for the vertical cone than the inclined cones. With increasing *Ha*, this difference in average velocity diminishes. At a high *Ra*, inclined cones show better heat transfer efficiency, while the opposite happens at low *Ra* for most values of *Ha*.

Acknowledgments

The authors would like to deeply appreciate the Department of Mathematics, Bangladesh University of Engineering and Technology, for supporting this research using supervision and providing computational facilities. They also thank the Mathematics Department, National University, Gazipur, for allowing the time and opportunity to conduct this research.

Author Contribution

Md. Abdul Alim: Concept, supervision, manuscript review. Saika Mahjabin: Literature review, simulation, results analysis, manuscript writing, and revision.

References

Ali MM, Akhter R and Alim MA. Performance of flow and heat transfer analysis of mixed convection in Casson fluid filled lid driven cavity including solid obstacle with magnetic impact. *SN Appl. Sci.* 2021; 3: 250.

Ashouri M, Shafii MB and Kokande HR. MHD natural convection flow in cavities filled with square solid blocks. *Int. J. Num. Methods Heat Fluid Flow*. 2014; 24(8): 1813-1830.

Bakar NA, Roslan R and Karimpour A. Magnetic field effect on mixed convection heat transfer in a Lid-driven rectangular cavity. *CFD Letters*. 2020; 12(1):13-21.

Bakhshan Y and Ashoori H. Analysis of a fluid behavior in a rectangular enclosure under the effect of magnetic field. *J. World Acad. Sci. Engg. Tech.* 2012*;* 6(1): 637-641.

Bhuiyan AH, Alim MA and Uddin MN. Effect of hartmann number on free convective flow in a square cavity with different positions of heated square block. *Int. J. Mat. Phy. Elect. Comp. Eng.* 2014; 8(2): 385-390.

Ciofalo, M. One-dimensional mixed MHD convection. In: *Thermo Fluid Dynamics*. UNIPA Springer Series. Springer, Cham. 2023.

Dechaumphai P. *Finite Element Method in Engineering.* 2nd ed. Chulalongkorn University Press, Bangkok; 1999.

Goud S, Yalana DR and Wakif A. Numerical analysis on the heat and mass transfer MHD flow characteristics of nanofluid on an inclined spinning disk with heat absorption and chemical reaction. *J. Heat Trans*. 2023, 52(2): 3615-3639.

Hossain SA, Alim MA and Saha SK. A Finite element analysis on MHD free convection flow in open square cavity containing heated circular cylinder. *Am. J. Comp. Mat.* 2015; 5(1): 41-54.

Kulacki FA, Davidson PF and Dunn JH. Convective heat transfer with electric and magnetic field. In: *Handbook of Single-Phase Convective Heat Transfer.* Kakac S, Shah RK and Aung W, eds., Wiley, NY; 1987.

Mahjabin S and Alim MA. Effect of hartmann number on free convective flow of MHD fluid in a square cavity with a heated cone of different orientation. *Am. J. Comp. Mat.* 2018; 8(4): 314-325

Moreau, M. *Magnetohydrodynamics*, Kluwer Acadamic, Dordrecht, The Netherlands. 1990.

Mythreye A. Chemical reaction effects on MHD free convection heat and mass transfer flow through a porous medium bounded by two vertical walls in the presence of radiation. *J. New Zealand Herpetology*. 2023, 12(1).

NASA https://www.grc.nasa.gov/www/k-12/airplane/lowhyper.html Retrieved on June 20, 2023.

Öztop FH and Al-Salem K. Effects of joule heating on MHD natural convection in non-isothermally heated enclosure. *J. Thermal Sci. Tech.* 2012; 32(1): 81-90.

Reddy JN. *An Introduction to Finite Element Method.* McGraw-Hill, NY. 1993.

Sathiyamoorthy M and Chamkha AJ. Natural convection flow under magnetic field in a square cavity for uniformly (or) linearly heated adjacent walls. *Int. J. Num. Methods Heat Fluid Flow.* 2012. 22(5): 677-698

Taghikhani MA and Chavoshi HR. Two dimensional MHD free convection with internal heating in a square cavity. *J. Therm. Energy Power Eng*. 2013; 2: 2-28.

Taylor C and Hood P. A Numerical solution of the navier-stokes equations using finite element technique. *J. Comp. Fluids.* 1973; 1(1): 73-89.

Vives C. and Perry C. Effects of magnetically damped convection during the controlled solidification of metals and alloys. *Int. J. Heat Mass Transf.* 1987; 30(3): 479-496.

Yang KT. Natural convection in enclosures. In: *Handbook of Single-Phase Convective Heat Transfer*, Kakac S, Shah RK and Aung W, eds., Wiley, NY. 1987.